MicroRNA-449a is a potential predictor of colitis-associated colorectal cancer progression

YUN FENG[1*], YU-WEI DONG[2*], YUN-NA SONG[3], JUN-HUA XIAO[4],
XING-YA GUO[2], WEI-LIANG JIANG[2] and LUN-GEN LU[1]

[1]Department of Gastroenterology, Shanghai General Hospital of Nanjing Medical University;
[2]Department of Gastroenterology, Shanghai General Hospital, Shanghai Jiao Tong University School of Medicine,
Shanghai 200080; [3]Department of Gastroenterology, Qihe People's Hospital, Dezhou, Shandong 251100;
[4]Department of Gastroenterology, Shanghai East Hospital, Tongji University School of Medicine, Shanghai 200120, P.R. China

Abstract. An early diagnosis of colitis-associated colorectal cancer (CAC) is important for its clinical management. However, it is currently difficult to distinguish the different stages of CAC development. MicroRNA dysregulation is common in human colorectal disorders, however little is known regarding whether miRNA affects tumor progression by regulating inflammation. In the present study, we identified a novel miRNA (miR-449a), the expression of which was significantly reduced in CAC tissues than in paired adjacent non-cancerous tissues (ANTs). Notably, the level of miR-449a was in a markedly decreased pattern during the neoplastic transformation of ulcerative colitis (UC)-to-CAC, as demonstrated by both clinical investigations and the experimental mouse model induced by AOM/DSS treatment. In addition, we observed that decreased miR-449a expression was associated with advanced T or N status, later clinical stage and poor histological differentiation of CAC. Mechanistic studies revealed that miR-449a inhibited the growth and metastasis of human colon cancer cells by directly binding to the 3'-UTR of Notch-1 and thereby, suppressed the activation of the Notch signaling pathway. Therefore, these findings provide strong evidence for the translational potential of miR-449a in the discrimination of patients with UC that is likely to progress into CAC, from those unlikely to progress, as well as in the prognosis and diagnosis of CAC.

Introduction

Colorectal cancer (CRC) is the third most common type of cancer and the second leading cause of cancer-related deaths worldwide (1). CRC can develop sporadically or in the background of several colonic disorders. Inflammatory bowel disease (IBD), including ulcerative colitis (UC) and Crohn's disease (CD), is characterized by the idiopathic, chronic and recurrent inflammatory conditions of the human bowel and is an important risk factor for developing CRC, thus called colitis-associated colorectal cancer (CAC) (2,3). UC patients with refractory and long-standing disease duration are reported to have a significantly increased cancer risk which increases with the earlier age of disease onset, the duration of the disease and the extent of colonic involvement (4,5). Eaden *et al* (6) estimated the cumulative cancer incidence for developing CAC as 2% at 10 years, 8% at 20 years and 18% at 30 years in patients affected by chronic colitis using a widely cited meta-analysis of 116 studies with age stratified data. A more recent study reported that the risk of CRC was 60% higher with extensive UC than in a without colitis-matched cohort of people (7). In contrast to UC, the role of CD in CRC risk remains controversial, and the majority of studies could not detect different incidence rates in comparison with the general population (8). Relative to sporadic CRC, CAC is usually linked to an earlier age of onset, a fast progressing course and a higher rate of mortality (9). Approximately 59% of CAC patients were deceased at the 5-year follow-up according to the statistics of Ording *et al* (10). These previous studies demonstrated that repeated colonic inflammation is a major contributing factor for CRC development.

Studies have revealed that the pathogenesis of CAC differs from the sporadic form. Though they share some disease mechanisms, such as mutations in oncogenes or tumor suppressors and genetic instabilities, differences in morphology and biological behaviors, timing and the sequence of genetic and epigenetic alterations are present (11). While most sporadic CRC demonstrates an 'adenoma-to-carcinoma'

profile, CAC arises through an 'inflammation-associated dysplasia-to-carcinoma' sequence, which, highlights important differences in their carcinogenic pathways (12). In either situation, the cancer develops from acquiring hallmark molecular alterations in the epithelium of the colon and rectum. Regrettably, 20 to 50% of UC patients with CAC were diagnosed with dysplasia only in the preoperative pathological diagnosis (13). This indicates the difficulty of surveillance for UC patients using colonoscopy. Thus, novel tumor markers for early clinical risk assessment and differential diagnosis are urgently required.

MicroRNAs (miRNAs) are endogenous small non-coding RNAs of 18 to 25 nucleotides in length that regulate gene expression through binding to the 3'-untranslated region (3'-UTR) of target messenger RNAs, either targeting the transcripts for degradation or blocking their translation. miRNAs are expressed in the human body in a cell- and tissue-specific manner and are crucial regulators of development and disease (14,15). The role of miRNAs in human sporadic CRC has been intensively studied in recent years. However, far less is known about their implications in UC-CAC development. Considering that the etiology of the disease is unclear, researchers are pursuing multiple independent approaches to identify sensitive, as well as specific biomarkers for early CAC (16). Though there are currently many biomarkers in development to discriminate IBD subtypes, there are few biomarkers for differentiating IBD progressors from non-progressors (17). As post-transcriptional modulators of intracellular signaling pathways, miRNAs are frequently found upregulated or downregulated during different stages of chronic inflammatory diseases. In the present study, we identified that miR-449a, which is a member of the miR-34/449 superfamily, was differentially expressed during the progression to carcinogenesis from UC, and may thus hold significant diagnostic potential in CAC.

Materials and methods

Patient information and tissue samples. Human colon mucosa samples were obtained from patients who received endoscopic biopsy or surgery at The Shanghai General Hospital and The Shanghai East Hospital between January 2007 and July 2017. In total, 41 cases of CAC tissues and paired adjacent non-cancerous tissues (ANTs) were collected from patients with pathologically diagnosed CAC (28 males, 13 females; mean age, 59.72±10.05 years) who had clear histories of chronic colitis suffering. Twenty-eight dysplasia-associated lesion or mass (DALM) samples (16 males, 12 females; mean age, 51.72±13.05 years) were collected and the dysplasia was defined according to the modified Vienna criteria (18). Sixty-three UC samples (33 males, 30 females; mean age, 45.58±10.96 years) and 49 CD samples (24 males, 25 females; mean age, 42.81±12.17 years) were from patients in the active stage of disease. The diagnosis of IBD was based on clinical, endoscopic and pathohistological criteria as previously described (19,20). Another 40 normal colorectal tissues obtained from people free of intestinal diseases (20 males, 20 females; mean age, 45.23±9.56 years) were used as a control. All biopsy specimens were fixed in liquid nitrogen or 10% formalin for analyses.

The present study was approved by the Ethics Committee of The Shanghai General Hospital and the Ethics Committee of The Shanghai East Hospital. The clinical study protocol strictly conformed to the ethical guidelines of the 1975 Declaration of Helsinki. Written informed consent was obtained from all patients.

Cell lines and cell culture. The human CRC cell lines SW620 and SW480 were obtained from the American Type Culture Collection (ATCC; Manassas, VA, USA) and grown in complete growth medium as recommended by the manufacturer. The cancer cells were maintained in a humidified 5% CO_2 atmosphere at 37˚C. Both cell lines were regularly authenticated by checking their morphology and confirming the absence of mycoplasma contamination (MycoAlert Mycoplasma Detection kit; Lonza, Rockland, ME, USA).

CAC animal model establishment. A cohort of 40 pathogen-free male Balb/c mice (6 weeks old, 18-20 g) was obtained from the Shanghai Institute of Materia Medica, Chinese Academy of Sciences (Shanghai, China). Every 5 mice were housed in an individual ventilated cage under controlled conditions of humidity (50±10%), lighting (12-h light/dark cycle) and temperature (25±2˚C) with pure water and a freely accessible pelleted basal diet. All protocols concerning laboratory animal use were submitted to, and validated by, the Animal Care Ethics Committee of Shanghai General Hospital.

Colitis-associated neoplasm was induced as previously described (21). In brief, animals were randomly divided into two groups (n=20). The 20 mice in the experimental group received intraperitoneally a single-dose injection of azoxymethane (AOM; Sigma-Aldrich, Munich, Germany) (10 mg/kg) on the first day. Dextran sodium sulfate (DSS; MP Biomedicals, Aurora, OH, USA) (4%) was dissolved in distilled water and administered in the first, third, fifth and seventh week. The same procedure was performed with intraperitoneal normal saline and drinking distilled water instead of the AOM/DSS treatment in the control group.

On the first day and at the end of weeks 1/7/9, 5 mice in each group were euthanized by decapitation and colon tissues were harvested and stored in 10% buffered formalin or at -80˚C in liquid nitrogen. The weight loss, stool consistency and bleeding were recorded daily to monitor the disease activity. Histological change was evaluated by hematoxylin and eosin (H&E) staining. The formalin-fixed distal colon tissues were embedded in paraffin blocks. Sliced sections (4 μm) were deparaffinized and rehydrated by a xylene-ethanol-water gradient system. H&E staining was then performed followed by a dehydration process.

In situ hybridization (ISH) and staining assessment. ISH analysis was performed using double-digoxigenin (DIG) labeled 2'O-methyl locked nucleic acid (LNA)-ZEN probes (Boster Biological Technology Co., Ltd., Wuhan, China) complimentary to miR-449a (5'-ACCAGCTAACAATACACTGCCA-3') along with a scrambled negative control probe (5'-GUAUUAUAG CCGAUUAACG-3'). Hybridization, washing, and scanning were performed according to previous studies (22).

A staining evaluation system incorporating the intensity and percentage of positive cells was conducted to assess the

miR-449a staining degree. The staining intensity was classified into four grades: 0, no staining; 1, weak; 2, moderate; 3, strong. The percentage of cells stained was graded as follows: 0, no staining; 1, <10%; 2, 10-50%; and 3, >50% cells. The final score was calculated by multiplying the grade for percentage staining by the grade for intensity. Scores of ≥4 were defined as positive staining and high expression. Each sample was evaluated by two experienced pathologists who were not aware of the experimental protocols.

Vectors and cell transfection. The DNA fragment of hsa-miR-449a was amplified from genomic DNA and inserted into the *Bam*HI/*Hin*dIII site of lentivirus expression vector pGCL (Shanghai GenePharma, Co., Ltd., Shanghai, China). An empty pGCL vector was used as a negative control. The Notch-1 expression vector was generated as previously described. In brief, the coding sequence of Notch-1 was amplified from cDNA and was then subcloned into a pcDNA3.1 plasmid (Thermo Fisher Scientific, Inc., Waltham, MA, USA). Cell transfection was performed with the Opti-MEM medium (Gibco; Thermo Fisher Scientific, Inc.) and Lipofectamine 2000 (Invitrogen; Thermo Fisher Scientific, Inc.) following the manufacturer's instructions.

Dual-luciferase reporter assay. Luciferase constructs were generated by ligating oligonucleotides containing the wild-type or mutant putative target site of the Notch-1 3'-UTR into the Psi-CHECK2 vector (Promega Corp., Madison, WI, USA) downstream of the luciferase gene. Human CRC cells were transfected with miR-449a expression vectors or the controls in combination with each individual psiCHECK2 luciferase vector. Cells were collected at 24 h after transfection, and firefly and *Renilla* luciferase activities were assessed using the Dual-Luciferase assay kit (Promega Corp.) (23).

Quantitative real-time RT-PCR. Total RNA was extracted from cells or tissues using TRIzol reagent (Invitrogen) following the manufacturer's instructions. The expression of miRNAs was quantified by two-step quantitative RT-PCR, beginning with first-strand cDNA synthesis using the One-step PrimeScript miRNA cDNA Synthesis kit (Takara, Kyoto, Japan), followed by quantitative real-time PCR amplification with the miScript SYBR-Green PCR kit (Takara). The quantitative SYBR-Green PCR kit (Qiagen, Hilden, Germany) was used to quantify the mRNA expression levels of genes in the Notch-1 signaling pathway. All reactions were run in triplicate on the MasterCycler Real-Time PCR Detection system (Eppendorf, Hamburg, Germany). The primer sequences used in the study are listed in Table I. The expression of miRNA was normalized to small nuclear RNA U6, while the other genes were normalized using the *GAPDH* gene. The fold change of miRNA/mRNA expression was calculated using the $2^{-\Delta\Delta Cq}$ method (24).

Western blot analysis. Total protein was extracted from the cells and measured with the bicinchoninic acid assay (BCA) kit (Beyotime Institute of Biotechnology, Shanghai, China). Whole protein lysates per lane (30 μg) were used to detect the indicated protein. The cell lysate was separated by 8% SDS-PAGE and then transferred to a olyvinylidene difluoride

Table I. Primers used in the study.

Oligo	Sequence
Notch-1	F: TCCTTCTACTGCGAGTGTCC
	R: TCGTTACAGGGGTTGCTGAT
Jagged-1	F: CTTCAATCTCAAGGCCAGCC
	R: CAGGCGAAACTGAAAGGCAG
Dll-4	F: TGTGGCAAACAGCAAAACCA
	R: CCGACACTCTGGCTTTTCACT
Hes-1	F: TTTGGATGCTCTGAAGAAAGATAGC
	R: CGGTACTTCCCCAGCACACTT
Hey-1	F: CGAGCTGGACGAGACCAT
	R: CTAGAGCCGAACTCAAGTTTCC
GAPDH	F: AGCGAGAACAATTACCCTGGGCAC
	R: ATTCTTGCCCTTCGCCTCTT

F, forward; R, reverse.

(PVDF) membrane at 320 mA for 2 h at 4˚C. The protein on the PVDF membrane was blocked with 5% fat-free milk in the PBST solution, cultured in primary anti-Notch1 antibody (1:1,000; cat. no. ab65297; Abcam, Cambridge, UK) and then incubated in the secondary rabbit anti-goat IgG-HRP antibody (1:2,000; cat. no. sc-2768; Santa Cruz Biotechnology, Dallas, TX, USA) for ~1-2 h at room temperature. PVDF membranes were washed and the signals of protein bands were visualized using ECL reagent (Promega Corp.). The densitometry scan of the western blotting was performed by Image-Pro Plus 6.0 (Media Cybernetics, Inc., Rockville, MD, USA). The resulting values of the proteins of interest were normalized to GAPDH.

Cell proliferation, migration and invasion assays. Cells ($3x10^3$) were plated in 96-well plates and allowed to grow for 24-120 h. Subsequently, the cells in each well were incubated with 10 μl of Cell Counting Kit-8 (CCK-8; Dojindo Laboratories, Kumamoto, Japan) at 37˚C for 4 h. The absorbance was assessed at 450 nm using a microplate reader. Each variant of these tests was performed in triplicate.

Cell migration was assessed with a wound-healing assay. Briefly, the cells were plated in a 6-well plate, and 24 h later, a scratch was made through the confluent cell monolayer using a pipette tip. The spread of the wound closure was photographed after 48 h.

For the invasion assays, cells ($1x10^5$) suspended in serum-free medium were plated in the upper chamber (8-μm pore size) coated with Matrigel (BD Biosciences, Flanklin Lakes, NJ, USA) and 600 μl of DMEM containing 10% FBS was added to the lower chamber to serve as a chemoattractant. Following 48 h, the non-invaded cells were gently removed with a cotton swab, while the cells located on the lower side of the chamber were fixed with 4% paraformaldehyde, stained with 0.1% crystal violet, air dried, photographed and quantified by counting them in five random fields using a light microscope (Leica Microsystems, Wetzalr, Germany). Each experiment was repeated at least three times.

Table II. Expression of miR-449a in different gastrointestinal diseases.

Gastrointestinal diseases	No. of patients	miR-449a expression		[a]P-value
		Low n (%)	High n (%)	
Ulcerative colitis	63	9 (14.3)	54 (85.7)	
DALM	28	11 (39.3)	17 (60.7)	
CAC	41	31 (75.6)	10 (24.4)	0.002[a]
Crohn's disease	49	23 (46.9)	26 (53.1)	
Normal control	40	34 (85.0)	6 (15.0)	

[a]P<0.05 indicates a significant relationship among the UC, DALM and CAC samples. The P-value was determined using a Chi-square test. UC, ulcerative colitis; DALM, dysplasia-associated lesion or mass; CAC, colitis-associated colorectal cancer.

Bioinformatics analysis. Integrated analysis of three miRNA target gene predication databases, including TargetScan (http://www.targetscan.org/vert_72/), Microcosm (https://www.microcosm.com/) and miRanda (http://www.microrna.org) was conducted to identify the number of miRNA-regulated target gene pairs. Only miRNAs shown to bind to the same region of the target 3'-UTR sequence in all the three programs were selected.

Statistical analysis. All data are presented as the mean ± standard deviation (SD) from at least three independent experiments with similar results. Statistical analyses were undertaken using SPSS version 19.0 software (IBM Corp., Armonk, NY, USA). Student's t-test was used to evaluate differences between two groups. One-way ANOVA test and Bonferroni post hoc test were used for evaluating differences among multiple groups. A value of P<0.05 was considered to indicate a statistically significant difference.

Results

The expression level of miR-449a is decreased in CAC tissues compared with the ANTs. Since the role of the miR-449 family members, which share the same seed region with the miR-34 family, has not been intensively studied in IBD or CAC, we first examined the expression of miR-449a, miR-449b and miR-449c in 41 pairs of CAC tissues and ANTs. Using RT-qPCR analysis, we found that miR-449a expression was significantly decreased in CAC tissues compared with the ANTs, whereas the levels of miR-449b and miR-449c did not exhibit a statistical difference between the CAC and ANTs (Fig. 1A). Furthermore, we performed an ISH analysis of miR-449a and confirmed that miR-449a was extensively expressed in adjacent mucosa, either with active or inactive inflammation, but not in malignant epithelial tissues (Fig. 1B).

Decreased miR-449a level is associated with CAC development. Subsequently, we investigated the expression of miR-449a in different stages of CAC progression and in CD and control samples by ISH staining. As shown in Table II, positive miR-449a expression was detected in 54/63 (85.7%) cases of UC samples and in 17/28 (60.7%) of DALM specimens, whereas CACs were predominately negative (75.6%)

for miR-449a staining. In addition, positive miR-449a staining was observed in 26/49 (53.1%) cases of CD and only 6/40 (15.0%) cases of normal controls free of intestinal diseases. Collectively, these data indicated that miR-449a was mostly inactive in normal mucosa, but was expressed at a high level during active intestinal inflammation. Notably, the expression of miR-449a was gradually decreased with advancing stages of UC-CAC development (Fig. 2).

Furthermore, we explored miR-449a expression in the 41 pairs of CAC samples to determine its clinical and pathological relevance. ISH analysis demonstrated that low expression of miR-449a was observed in 31/41 (75.6%) cases of CAC patients, whereas high expression of miR-449a was observed in only 10/41 (24.4%) of the patients. Clinicopathological investigations revealed that decreased expression level of miR-449a was associated with local invasion (P=0.001), lymph node metastasis (P=0.024), AJCC stage (P=0.021) and histological grade (P=0.017) of the colitis-associated tumors, but not with patient age (P=0.232), sex (P=0.564) or tumor location (P=0.191) (Table III). These results indicated that suppression of miR-449a was closely linked with the aggressive parameters of CAC and may thus represent a potential predictive factor of CAC progression.

Colonic expression of miR-449a is also decreased during CAC tumorigenesis in AOM/DSS-treated mice. For further validation, an AOM/DSS-induced CAC mouse model was established and RNA samples were extracted from distal colorectal mucosa on the first day (negative control) and at the end of week 1 (colitis), week 7 (dysplasia) and week 9 (cancer). Morphological and histological evaluation revealed that there was significant colonic inflammatory infiltration and active colitis by the end of the first week; while at the 7th week time-point, neoplastic transformation was observed in the distal colon. Lastly, by the end of week 9, high grade dysplasia and carcinoma were observed in the entire intestinal tract (Fig. 3A, upper and middle panels). Subsequently, RT-qPCR and ISH analyses were used to assess the expression level of miR-449a. As anticipated, miR-449a was markedly increased in the inflammatory mucosa compared with the normal colon, and then gradually declined during the course of colitis-to-colorectal neoplasm (Fig. 3B). miR-449a exhibited strong to moderate expression in inflammatory tissues
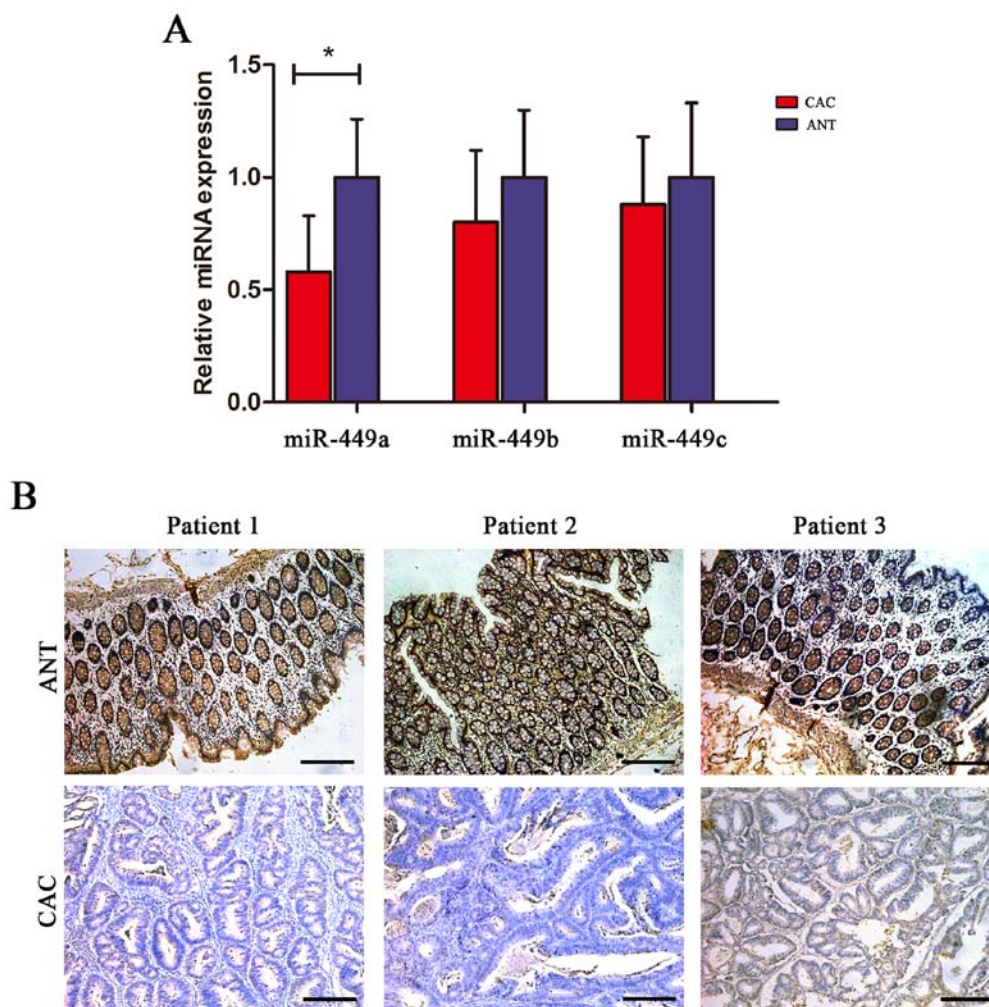
Figure 1. Expression of miR-449a is significantly lower in CAC tissues than in the paired adjacent non-cancerous tissues (ANTs). (A) RT-qPCR analysis of the expression of miR-449 family members in patient CAC tissues and ANTs. *P<0.05. Data are expressed as the mean ± SD. (B) Representative *in situ* hybridization (ISH) analysis of the expression of miR-449a in 3 pairs of CAC and ANTs. Scale bar, 100 μm. CAC, colitis-associated colorectal cancer.
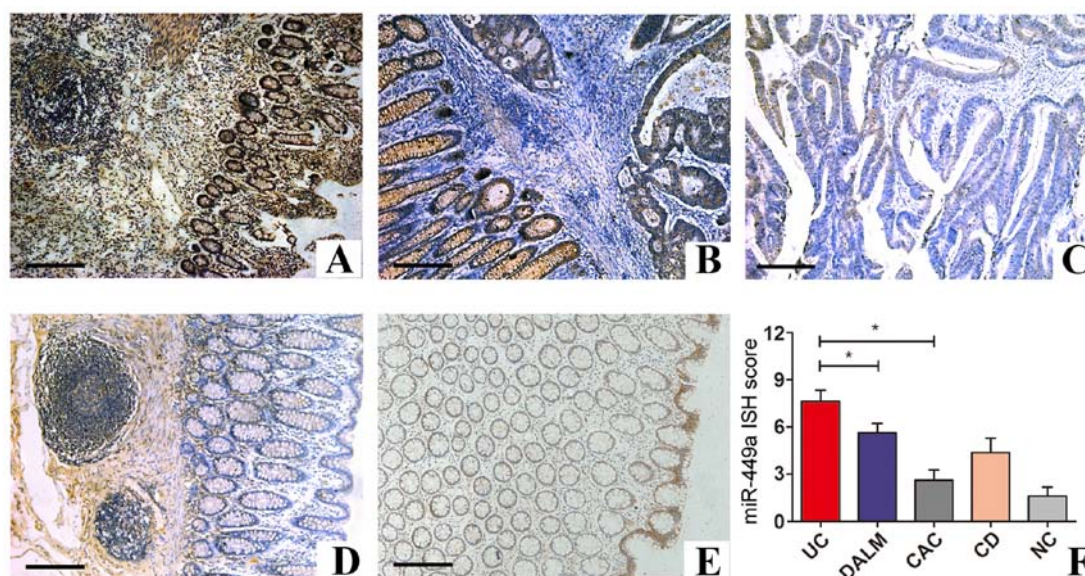

Figure 2. Assessment of the expression of miR-449a in different colorectal diseases. Representative *in situ* hybridization (ISH) analysis of miR-449a expression in human (A) UC tissues, (B) dysplasia-associated lesion or mass samples, (C) colitis-associated colorectal cancer tissues, (D) CD tissues, and (E) normal colon tissues. (F) Evaluation of miR-449 ISH staining. *P<0.05. Scale bar, 100 mm. Data are presented as the mean ± SD. UC, ulcerative colitis; CD, Crohn's disease.

Table III. Correlation between clinicopathological characteristics and the expression of miR-449a in patients with CAC.

| Characteristics | No. of patients (%) | miR-449a expression | | [a]P-value |
		High n=10 (%)	Low n=31 (%)	
Age, years				
<55	17 (41.5)	4 (40.0)	13 (41.9)	0.232
≥55	24 (58.5)	6 (60.0)	18 (58.1)	
Sex				
Male	28 (68.3)	7 (70.0)	21 (67.7)	0.564
Female	13 (31.7)	3 (30.0)	10 (32.3)	
Tumor location				
Left	30 (73.2)	7 (70.0)	23 (74.2)	0.191
Right	11 (26.8)	3 (30.0)	8 (25.8)	
pT status				
T1/T2	14 (34.1)	8 (80.0)	6 (19.4)	0.001[a]
T3/T4	27 (65.9)	2 (20.0)	25 (80.6)	
pN status				
Absent	25 (61.0)	8 (80.0)	17 (54.8)	0.024[a]
Present	16 (39.0)	2 (20.0)	14 (45.2)	
AJCC stage				
I/II	24 (58.5)	8 (80.0)	16 (51.6)	0.021[a]
III/IV	17 (41.5)	2 (20.0)	15 (48.4)	
Histology				
Well/moderate	31 (75.6)	9 (90.0)	22 (71.0)	0.017[a]
Poor	10 (24.4)	1 (10.0)	9 (29.0)	

[a]Statistically significant. CAC, colitis-associated colorectal cancer.

and weak or negative staining in CAC tissues (Fig. 3A, lower panel). Thus, these data demonstrated dynamic expression of miR-449a during the tumorigenic course of CAC formation in a rodent model, which, is in line with the clinical observations.

miR-449a inhibits CAC growth and invasion by targeting Notch-1. To establish the role of miR-449a in colon cancer, we first constructed miR-449a expression vectors as well as the empty control vectors and transfected them into the human CRC cell lines SW620 and SW480 (Fig. 4A displays the transfection efficiency). Subsequently, we tested the effects of miR-449a on CRC cell proliferation by CCK-8 assay. Overexpression of miR-449a in two CRC cell lines significantly inhibited the proliferation rate of tumor cells *in vitro*, whereas transfection of the empty controls revealed no significant effects on cell proliferation (Fig. 4B). We next investigated the influence of miR-449a on CRC cell migration and invasion. Using a Transwell assay, we observed that significantly less miR-449a-overexpressed SW480 or SW620 cells invaded through the Matrigel and migrated to the lower surface of the filter, compared with the respective controls (Fig. 4C), indicating that miR-449a effectively reduced the invasive capability of CRC cells. Furthermore, the wound-healing assay revealed that miR-449a significantly inhibited cell migration (Fig. 4D). Collectively, these results

demonstrated that miR-449a may act as an important tumor suppressor in CRC, as well as CAC.

Subsequently, we explored the mechanism by which suppression of miR-449a during CAC development promoted tumor growth. After searching three miRNA prediction databases (TargetScan, Microcosm and miRanda), a putative miR-449a binding site in the 3'-UTR of Notch-1, a well-characterized oncogene in human CRC, was identified. Previous evidence has demonstrated that activated Notch signaling is maintained throughout CRC tumorigenesis (25). In addition, enhanced levels of Notch-1 have been associated with progression, tumor grade and metastasis (26). Using the miRNA target prediction programs, we found that the 3'-UTRs of Notch-1 mRNAs contain conserved miR-449a binding sites, which are highly conserved among human, mouse, rat, chimpanzee, dog and chicken species (Fig. 5A). We thus conducted a dual-luciferase reporter assay by constructing luciferase reporter constructs containing the wild-type or mutant Notch-1 3'-UTR (Fig. 5B) and co-transfected them with miR-449a expression vectors or the empty controls into target cells. We found that overexpression of miR-449a markedly reduced the luciferase activity of the wild-type 3'-UTR of Notch-1, but not the mutant reporter constructs, in both SW620 and SW480 cells (Fig. 5C). Further PCR and western blot verifications confirmed the direct inhibition of miR-449a
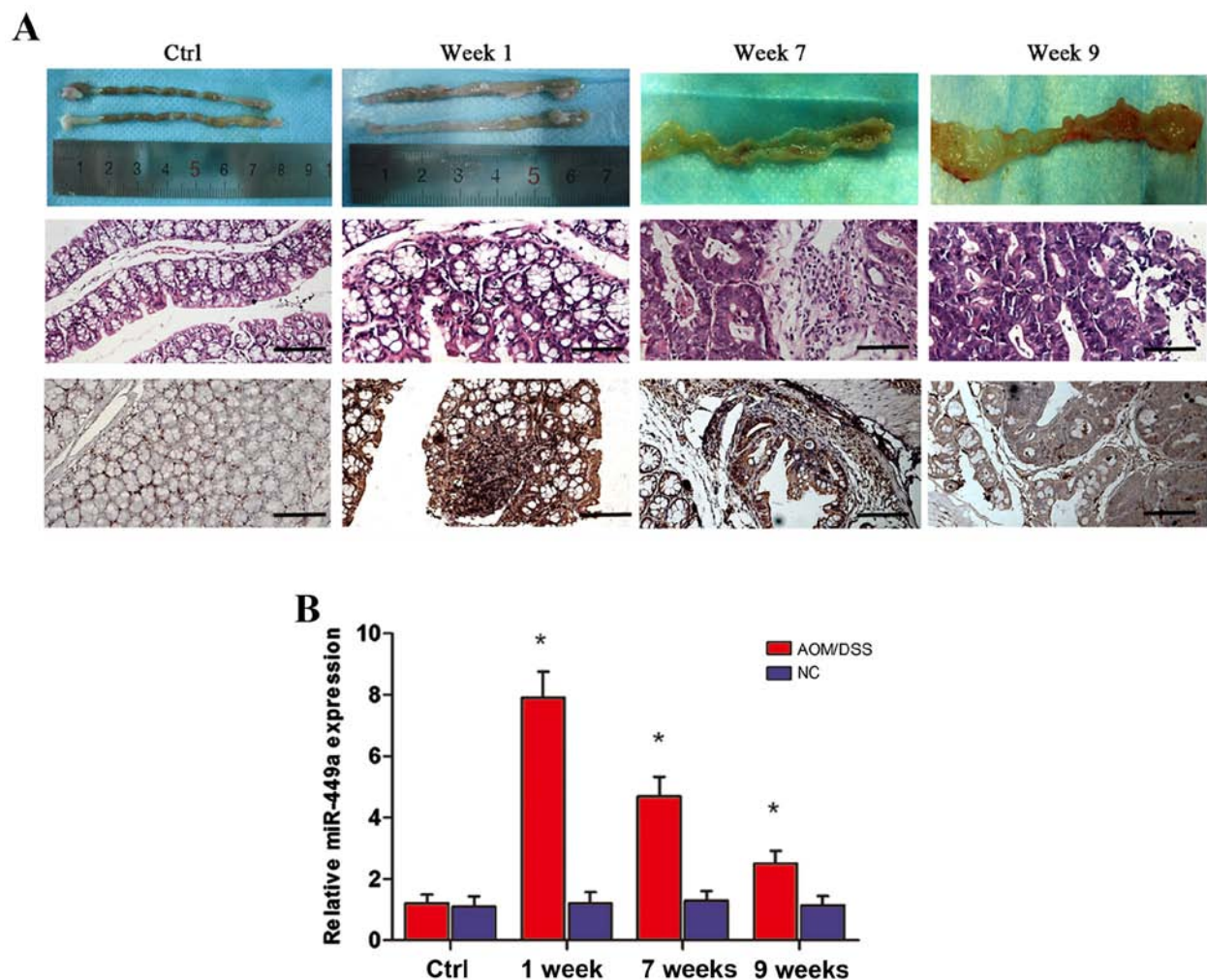
Figure 3. Decreased miR-449a expression during CAC tumorigenesis in the AOM/DSS model. (A) Representative histological images (upper panels), H&E staining (middle panels) and *in situ* hybridization (ISH) of miR-449a (lower panels) of the distal colorectal tissues from AOM/DSS-treated mice at different time-points. (B) RT-qPCR analysis of miR-449a expression in mice colon tissues. *P<0.05, 1st week vs. the control; 7th week vs. the 1st week; and 9th week vs. the 7th week. AOM, azoxymethane; DSS, dextran sodium sulfate.

on the gene and protein levels of Notch-1 expression (Fig. 5D). Additionally, we examined the influence of miR-449a on intracellular Notch signaling. It was observed that Jagged-1, Dll-4, Hes-1 and Hey-1, which are key factors of the canonical Notch pathway and are critical regulators of CRC/CAC metastasis and angiogenesis (27), were all significantly decreased after miR-449a overexpression in SW620 and SW480 cells. However, through the restoration of Notch-1 expression, these effects were partially reversed (Fig. 5E). Lastly, we performed *in vitro* studies and confirmed that Nocth-1 restoration could also reverse the inhibition of miR-449a on CRC cell proliferation, migration and invasion (Fig. 4B-D). Therefore, our findings indicated that miR-449a inhibited the tumorigenesis of CAC by directly targeting Notch-1 and its downstream oncogenic effectors, and the decreased miR-449a level was supposed to be an important factor for sustained activation of the Notch signaling in CAC progression.

Discussion

It is widely accepted that perpetuated intestinal inflammation markedly increases the risk of cancer. However, the detailed

mechanisms concerning the biological and genetic alterations that endow malignant cells with growth and motility advantages over normal epithelial cells have not been comprehensively elucidated. In the present study, we identified a novel miRNA, miR-449a, that was expressed in a decreased pattern during the neoplastic transformation of CAC. In addition, we demonstrated that miR-449a served its tumor-suppressor functions by inhibiting the Notch-1 signaling pathway. These findings may aid in uncovering the molecular events that drive CAC progression, and may indicate the broad clinical prospects for miR-449a in the management of human CAC.

It is known that miRNA genomic clusters are often co-transcribed as related miRNAs, which share the same seed region or belong to functionally related miRNA families. A typical example is given by the miR-34/449 superfamily, which exhibits extensive genomic redundancy by encompassing six homologous miRNAs (miR-34a, miR-34b/c and miR-449a/b/c) located on three distinct genomic loci (28). While the tumor suppressor role of miR-34 has been largely established, the effects of the miR-449 family members have not been addressed in human CRC, as well as CAC (29,30). Therefore, we first determined the expression of miR-449a,
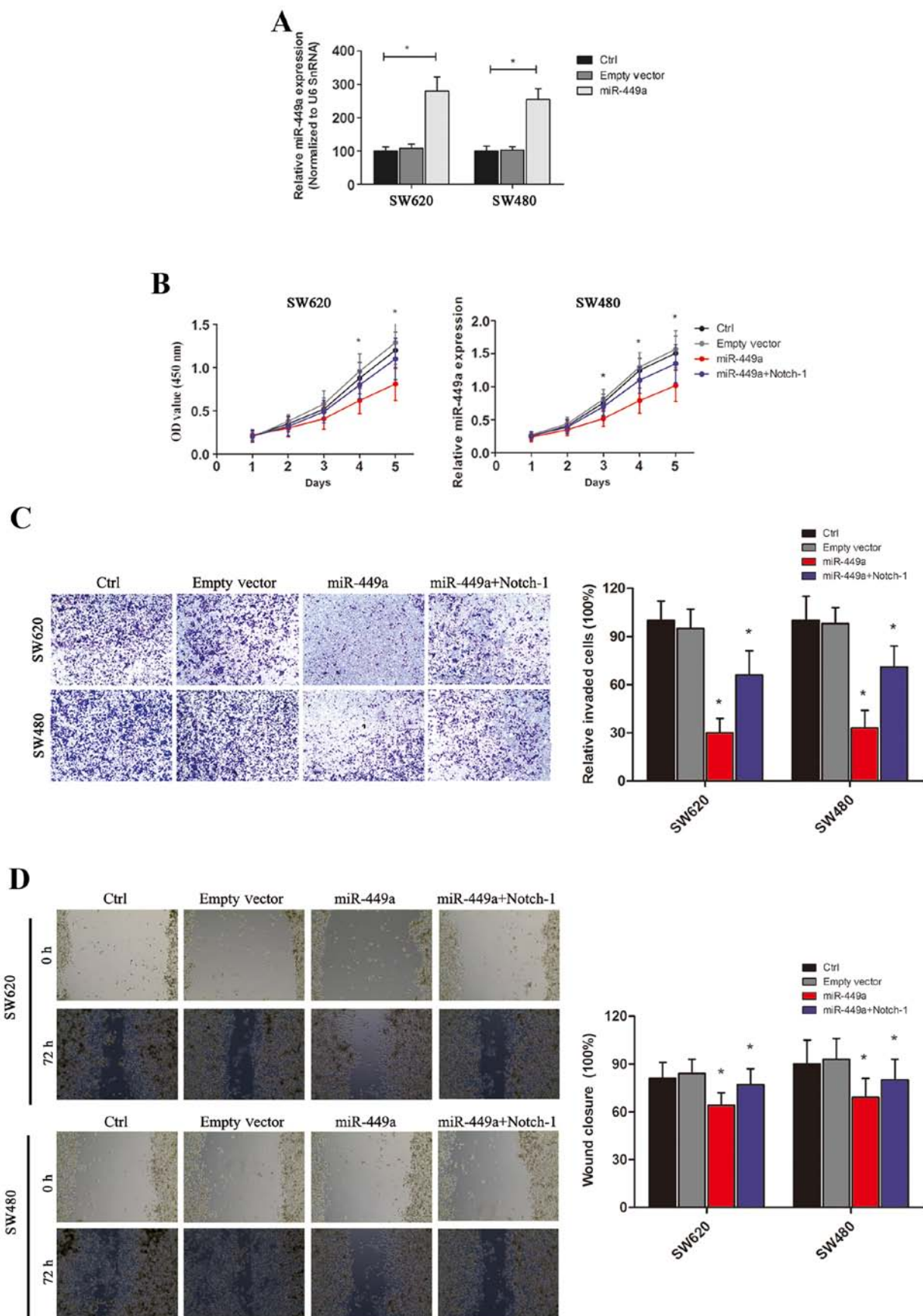
Figure 4. miR-449 inhibits the proliferation, invasion and migration of human colon cancer cells. (A) RT-qPCR verification of the transfection efficiencies of miR-449a expression vectors in SW620 and SW480 cells. (B) CCK-8 analysis of the proliferation of the control, empty vector-, miR-449a expression vector-, and miR-449a and Notch-1 expression vector-transfected SW620 or SW480 cells. (C) Transwell analysis of cell invasion. A Transwell assay was used to estimate the effects of miR-449a on the invasion of CRC cells. The number of cells that invaded through the membrane was counted and compared in the diagrams. Original magnification x20. (D) A wound healing assay was performed to determine the effects of miR-449a on cell migration ability. The percentage of wound closure was compared in the diagrams. *P<0.05. All data are presented as the mean ± SD.
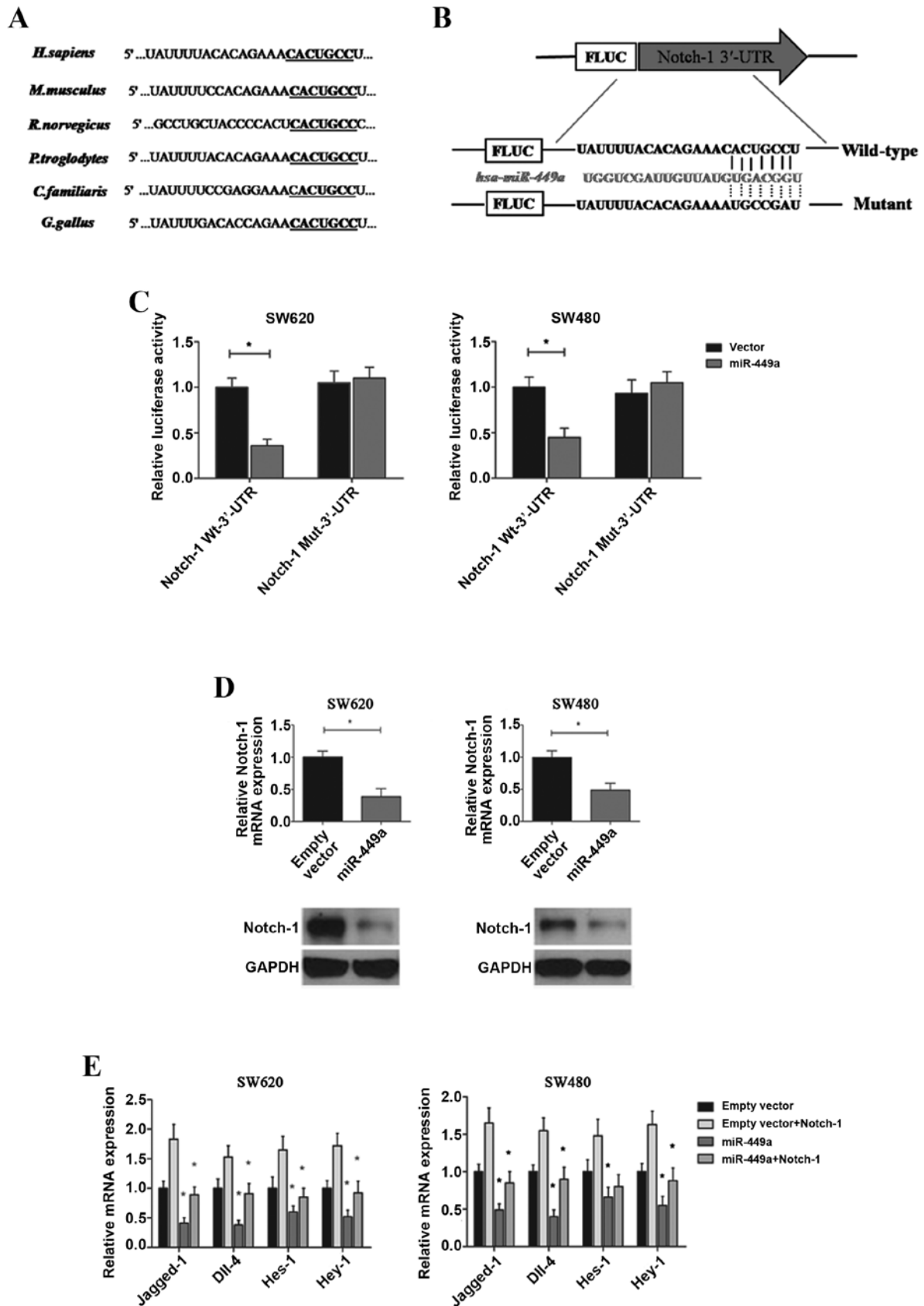
Figure 5. miR-449a suppresses the Notch signaling pathway by directly targeting the 3'-UTR of Notch-1. (A) The sequences on Notch-1 3'-UTR for potential binding with miR-449a were aligned among human (*H. sapiens*), mouse (*M. musculus*), rat (*R. norvegicus*), chimpanzee (*P. troglodytes*), dog (*C. familiaris*) and chicken (*G. gallus*) species. Seed sequences were highlighted and underlined. (B) A human Notch-1 3'-UTR fragment containing the wild-type or mutant miR-449a-binding sequence was cloned downstream to the luciferase reporter gene. (C) The luciferase activity of wild-type or mutant Notch-1 3'-UTR in SW620 and SW480 cells transfected with miR-449a expression vectors or empty controls. (D) RT-qPCR and western blot analysis of the effects of miR-449a on Notch-1 expression in SW620 and SW480 cells. GAPDH was used as internal control. (E) miR-449a overexpression significantly inhibited the expression of key effectors in the Notch-1 signaling pathway, while restoration of Notch-1 expression could partially reverse the inhibition. $^*P<0.05$. Data are expressed as the mean ± SD.

miR-449b and miR-449c in colon samples obtained from CAC patients with a clear history of chronic colitis, and we determined that only miR-449a was significantly lower in CAC tissues than in ANTs. Further ISH staining demonstrated that miR-449a was markedly activated in inflamed UC tissues, and expressed increasingly less in DALM and CAC samples. Notably, high expression of miR-449a was detected in most UC tissues (85.7%), however, half the CD samples expressed miR-449a at low levels (46.9%), which is probably due to the different immunoreaction types and inflammatory activities between the two subtypes of IBD (31,32). Specifically, these findings also identified miR-449a as a molecular candidate for the discrimination of IBD subtypes.

Long-term UC patients are known to have a high risk for developing CRC compared with the general population. The current standard of care for surveillance of chronic UC patients largely depends on routine colonoscopy examination (33,34), it is therefore important to identify and develop biomarkers for stratifying the patients who undergo repeated colorectal inflammation and have a relatively high cancer risk. Since CAC progresses in a step-wise fashion, which is usually characterized as colitis negative for dysplasia (NEG), indefinite for dysplasia (IND), low-grade dysplasia (LGD) and high-grade dysplasia (HGD) cancer, new molecular markers detecting the premalignant lesions to discriminate UC progressors from non-progressors are useful for CAC prevention (35,36). An ideal biomarker for diagnosis should be highly specific, sensitive and less invasive. Previous research has demonstrated that miRNAs exhibit unique expression profiles in different tumor types and are critical for the initiation and progression of human cancers (37). The crucial functions of miRNAs in tumorigenesis have promoted intensive research into miRNA-based diagnostic and therapeutic applications. In the present study, for the first time, we identified miR-449a as a novel CAC-associated miRNA that was expressed in close relevance with patient disease status during UC-CAC progression. Notably, a CAC rodent model established by AOM/DSS induction further confirmed that miR-449a followed a linear pathway of downregulation in CAC carcinogenesis. Furthermore, our clinicopathological investigation on a cohort of 41 CAC patients revealed that decreased miR-449a expression was also associated with advanced T or N status, later clinical stage, and poor histological differentiation of tumors. These data collectively provided strong evidence for the translational potential of miR-449a in the prediction, diagnosis and prognosis of human CAC.

Cancer formation can be attributed to the dysfunction of cellular signaling transduction. The Notch pathway, which is highly conserved across evolution, is one of the master regulators of colonic epithelium development, differentiation and cell proliferation and apoptosis (38). Abnormal Notch signaling along with genetic or epigenetic mutations has been highly noted in a variety of gastrointestinal pathologies, including mucosal inflammation and tumorigenesis (25,39). Modulation of Notch signaling therefore, offers an approach for CRC treatment (40). In the present study, we revealed that miR-449a is a novel Notch-targeting miRNA, by directly binding to the 3'-UTR of Notch-1, a major receptor of signaling; miR-449a markedly suppressed Notch-1 expression at the gene and protein levels. It has been documented that Notch-1 elevation was positively associated with tumor growth, metastasis and poor clinical outcomes in human CRC, which could be related to inhibition of apoptosis promoted by Notch-1 (41). In the present study, we demonstrated that the key effectors of the canonical Notch pathway, such as Jagged-1, Dll-4, Hes-1 and Hey-1, were all significantly suppressed by miR-449a overexpression and were partially reversed after Notch-1 restoration. Thus, miR-449a suppresses CAC via the specific regulation of the Notch signaling cascade.

In conclusion, the present study has characterized miR-449a as a novel tumor suppressor miRNA by targeting the Notch pathway. The expression of miR-449a was gradually decreased during the progression of CAC, which, renders it a promising predictive and diagnostic factor for UC-CAC patients. Further large-scale clinical investigations and long-term prognostic analyses are still needed for the verification of the clinical and therapeutic application of miR-449a in human CAC.

Availability of data and materials

The datasets used during the present study are available from the corresponding author upon reasonable request.

Authors' contributions

YF, YWD, YNS and JHX performed the experiments, LGL designed the study, XYG and WLJ prepared and wrote the study. All authors read and approved the manuscript and agree to be accountable for all aspects of the research in ensuring that the accuracy or integrity of any part of the work are appropriately investigated and resolved.

Ethics approval and consent to participate

This study was approved by the Ethics Committee of Shanghai General Hospital and the Ethics Committee of Shanghai East Hospital. The clinical study protocol strictly conformed to the ethical guidelines of the 1975 Declaration of Helsinki. Written informed consent was obtained from all of the patients. All protocols concerning laboratory animal use were validated by the Animal Care Ethics Committee of Shanghai General Hospital.

Patient consent for publication

Not applicable.

Competing interests

The authors declare that they have no competing interests.

References

1. Siegel RL, Miller KD and Jemal A: Cancer statistics, 2017. CA Cancer J Clin 67: 7-30, 2017.
2. Abraham C and Cho JH: Inflammatory bowel disease. N Engl J Med 361: 2066-2078, 2009.
3. Kaplan GG and Ng SC: Globalisation of inflammatory bowel disease: Perspectives from the evolution of inflammatory bowel disease in the UK and China. Lancet Gastroenterol Hepatol 1: 307-316, 2016.
4. Fumery M, Dulai PS, Gupta S, Prokop LJ, Ramamoorthy S, Sandborn WJ and Singh S: Incidence, risk factors, and outcomes of colorectal cancer in patients with ulcerative colitis with low-grade dysplasia: A systematic review and meta-analysis. Clin Gastroenterol Hepatol 15: 665-674.e5, 2017.
5. Rogler G: Chronic ulcerative colitis and colorectal cancer. Cancer Lett 345: 235-241, 2014.
6. Eaden JA, Abrams KR and Mayberry JF: The risk of colorectal cancer in ulcerative colitis: A meta-analysis. Gut 48: 526-535, 2001.
7. Herrinton LJ, Liu L, Levin TR, Allison JE, Lewis JD and Velayos F: Incidence and mortality of colorectal adenocarcinoma in persons with inflammatory bowel disease from 1998 to 2010. Gastroenterology 143: 382-389, 2012.
8. Sebastian S, Hernández V, Myrelid P, Kariv R, Tsianos E, Toruner M, Marti-Gallostra M, Spinelli A, van der Meulen-de Jong AE, Yuksel ES, et al: Colorectal cancer in inflammatory bowel disease: Results of the 3rd ECCO pathogenesis scientific workshop (I). J Crohns Colitis 8: 5-18, 2014.
9. Yashiro M: Ulcerative colitis-associated colorectal cancer. World J Gastroenterol 20: 16389-16397, 2014.
10. Ording AG, Horváth-Puhó E, Erichsen R, Long MD, Baron JA, Lash TL and Sørensen HT: Five-year mortality in colorectal cancer patients with ulcerative colitis or Crohn's disease: A nationwide population-based cohort study. Inflamm Bowel Dis 19: 800-805, 2013.
11. Itzkowitz SH and Yio X: Inflammation and cancer IV. Colorectal cancer in inflammatory bowel disease: The role of inflammation. Am J Physiol Gastrointest Liver Physiol 287: G7-G17, 2004.
12. Luo C and Zhang H: The role of proinflammatory pathways in the pathogenesis of colitis-associated colorectal cancer. Mediators Inflamm 2017: 5126048, 2017.
13. Kinugasa T and Akagi Y: Status of colitis-associated cancer in ulcerative colitis. World J Gastrointest Oncol 8: 351-357, 2016.
14. Mendell JT and Olson EN: MicroRNAs in stress signaling and human disease. Cell 148: 1172-1187, 2012.
15. Ambros V: MicroRNAs and developmental timing. Curr Opin Genet Dev 21: 511-517, 2011.
16. Saraggi D, Fassan M, Mescoli C, Scarpa M, Valeri N, Michielan A, D'Incà R and Rugge M: The molecular landscape of colitis-associated carcinogenesis. Dig Liver Dis 49: 326-330, 2017.
17. Romano M, DE Francesco F, Zarantonello L, Ruffolo C, Ferraro GA, Zanus G, Giordano A, Bassi N and Cillo U: From inflammation to cancer in inflammatory bowel disease: Molecular perspectives. Anticancer Res 36: 1447-1460, 2016.
18. Schlemper RJ, Riddell RH, Kato Y, Borchard F, Cooper HS, Dawsey SM, Dixon MF, Fenoglio-Preiser CM, Fléjou JF, Geboes K, et al: The Vienna classification of gastrointestinal epithelial neoplasia. Gut 47: 251-255, 2000.
19. Ungaro R, Mehandru S, Allen PB, Peyrin-Biroulet L and Colombel JF: Ulcerative colitis. Lancet 389: 1756-1770, 2017.
20. Torres J, Mehandru S, Colombel JF and Peyrin-Biroulet L: Crohn's disease. Lancet 389: 1741-1755, 2017.
21. Bader JE, Enos RT, Velázquez KT, Carson MS, Nagarkatti M, Nagarkatti PS, Chatzistamou I, Davis JM, Carson JA, Robinson CM, et al: Macrophage depletion using clodronate liposomes decreases tumorigenesis and alters gut microbiota in the AOM/DSS mouse model of colon cancer. Am J Physiol Gastrointest Liver Physiol 314: G22-G31, 2018.
22. Fang Z, Yin S, Sun R, Zhang S, Fu M, Wu Y, Zhang T, Khaliq J and Li Y: miR-140-5p suppresses the proliferation, migration and invasion of gastric cancer by regulating YES1. Mol Cancer 16: 139, 2017.
23. Shen J, Zhang S, Li Y, Zhang W, Chen J, Zhang M, Wang T, Jiang L, Zou X, et al: p14ARF inhibits the functions of adenovirus E1A oncoprotein. Biochem J 434: 275-285, 2011.
24. Livak KJ and Schmittgen TD: Analysis of relative gene expression data using real-time quantitative PCR and the $2^{-\Delta\Delta C_T}$ method. Methods 25: 402-408, 2001.
25. Vinson KE, George DC, Fender AW, Bertrand FE and Sigounas G: The Notch pathway in colorectal cancer. Int J Cancer 138: 1835-1842, 2016.
26. Li G, Zhou Z, Zhou H, Zhao L, Chen D, Chen H, Zou H, Qi Y, Jia W and Pang L: The expression profile and clinicopathological significance of Notch1 in patients with colorectal cancer: A meta-analysis. Future Oncol 13: 2103-2118, 2017.
27. Lamy M, Ferreira A, Dias JS, Braga S, Silva G and Barbas A: Notch-out for breast cancer therapies. N Biotechnol 39: 215-221, 2017.
28. Mercey O, Popa A, Cavard A, Paquet A, Chevalier B, Pons N, Magnone V, Zangari J, Brest P, Zaragosi LE, et al: Characterizing isomiR variants within the microRNA-34/449 family. FEBS Lett 591: 693-705, 2017.
29. Wang LG, Ni Y, Su BH, Mu XR, Shen HC and Du JJ: MicroRNA-34b functions as a tumor suppressor and acts as a nodal point in the feedback loop with Met. Int J Oncol 42: 957-962, 2013.
30. Jiang L and Hermeking H: miR-34a and miR-34b/c suppress intestinal tumorigenesis. Cancer Res 77: 2746-2758, 2017.
31. Wallace KL, Zheng LB, Kanazawa Y and Shih DQ: Immunopathology of inflammatory bowel disease. World J Gastroenterol 20: 6-21, 2014.
32. Peyrin-Biroulet L, Panés J, Sandborn WJ, Vermeire S, Danese S, Feagan BG, Colombel JF, Hanauer SB and Rycroft B: Defining disease severity in inflammatory bowel diseases: Current and future directions. Clin Gastroenterol Hepatol 14: 348-354.e7, 2016.
33. Hata K, Kishikawa J, Anzai H, Shinagawa T, Kazama S, Ishii H, Nozawa H, Kawai K, Kiyomatsu T, Tanaka J, et al: Surveillance colonoscopy for colitis-associated dysplasia and cancer in ulcerative colitis patients. Dig Endosc 28: 260-265, 2016.
34. Feuerstein JD and Cheifetz AS: Ulcerative colitis: Epidemiology, diagnosis, and management. Mayo Clinic Proc 89: 1553-1563, 2014.
35. Bressenot A, Cahn V, Danese S and Peyrin-Biroulet L: Microscopic features of colorectal neoplasia in inflammatory bowel diseases. World J Gastroenterol 20: 3164-3172, 2014.
36. Chen R, Lai LA, Brentnall TA and Pan S: Biomarkers for colitis-associated colorectal cancer. World J Gastroenterol 22: 7882-7891, 2016.
37. Lujambio A and Lowe SW: The microcosmos of cancer. Nature 482: 347-355, 2012.
38. de Santa Barbara P, van den Brink GR and Roberts DJ: Development and differentiation of the intestinal epithelium. Cell Mol Life Sci 60: 1322-1332, 2003.
39. Fazio C and Ricciardiello L: Inflammation and Notch signaling: A crosstalk with opposite effects on tumorigenesis. Cell Death Dis 7: e2515, 2016.
40. Takebe N, Nguyen D and Yang SX: Targeting notch signaling pathway in cancer: Clinical development advances and challenges. Pharmacol Ther 141: 140-149, 2014.
41. Chu D, Zhang Z, Zhou Y, Wang W, Li Y, Zhang H, Dong G, Zhao Q and Ji G: Notch1 and Notch2 have opposite prognostic effects on patients with colorectal cancer. Ann Oncol 22: 2440-2447, 2011.